

Articles

Otteliones A and B: Potently Cytotoxic
4-Methylene-2-cyclohexenones from *Ottelia alismoides*Seif-Eldin N. Ayyad,^{*,†} Andrew S. Judd,[‡] W. Thomas Shier,[§] and Thomas R. Hoye^{*,‡}Chemistry Department, Faculty of Science, Mansoura University, New Dammiatta, Egypt, and
Departments of Chemistry and Medicinal Chemistry, University of Minnesota,
Minneapolis, Minnesota 55455

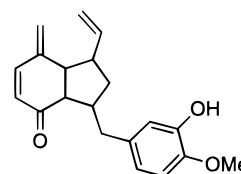
Received October 10, 1997 (Revised Manuscript Received June 9, 1998)

Two diastereomeric 4-methylene-2-cyclohexenones, otteliones A and B (**1A** and **1B**), have been isolated from the freshwater plant *Ottelia alismoides* collected in the Nile Delta, Egypt. These natural products show remarkable in vitro cytotoxicity against various cancer cell lines. Ottelione B proved to have a constitution identical to that of the known (constitution only) ottelione A. The relative configurations of both **1A** and **1B** were studied by NOE and by the combination of molecular modeling and ¹H NMR coupling constant analysis. A unique relative configurational assignment (1 α ,3 β ,3 $\alpha\beta$,7 α) was deduced for **1B**; **1A** was assigned one of two alternative diastereomers (1 α ,3 α ,3 α ,7 α or 1 α ,3 α ,3 $\alpha\beta$,7 $\alpha\beta$).

Ottelia alismoides is a little-studied, freshwater plant that grows partially submerged with rosetted, broadly cordate, floating leaves on long petioles.¹ Its distribution in Egypt is rare, but it blooms annually in rice fields and irrigation channels during the summer months. In the present study, *O. alismoides* was collected from the irrigation channels of the Nile Delta in Egypt during August 1996.

Our interest in this species was prompted by initial reports of its antitubercular effect.² The crude cyclohexane extracts of whole dried *O. alismoides* showed significant growth inhibition [50% growth inhibition (GI₅₀) \approx 1 μ g/mL] in two cultured mouse tumor cell lines (NIH3T3 and SSVNIH3T3). Following silica gel chromatography of these extracts, two chromatographically and spectroscopically similar compounds (**1A** and **1B**, which we now name otteliones A and B, respectively) were isolated in approximately equal amounts. The first to elute, ottelione A (**1A**), was identical with the sample reported in the patent literature by Leboul and Provost at Rhone-Poulenc Rorer, which was deduced to have the interesting constitution **1**.³ From similarities in chemical shifts and resonance multiplicities in their proton and carbon NMR spectra as well as their nearly identical IR spectra, it was apparent that the second, previously unknown compound, ottelione B (**1B**), was a stereoisomer of ottelione A (**1A**).

The only other previously reported compounds having related substructures⁴ are the regioisomeric hydrindene derivatives **2a** and **2b**⁵ and the parent 4-methylene-2-cyclohexenone (**3**).⁶ Regioisomers **2a** and **2b** were pre-

**1A 1B**

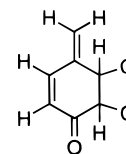
pared by a pyrolysis reaction at 600 °C; the preferred synthesis of **3** relies on an acid-catalyzed dehydration (1 N H₂SO₄, 100 °C) as the last step. The forcing conditions used in each of these preparations suggest that these dienones are kinetically protected toward isomerization to their more stable aromatic (*p*-cresol) tautomers.⁷

In addition to having unique structural features, these compounds have shown interesting biological activity. Ottelione A (**1A**) had been shown to inhibit tubulin polymerization into microtubules—the same mitotic event that is inhibited by colchicine, vincristine, and vinblastine.³ It was also shown to inhibit a doxorubicin resistant

(2) Li, H.; Li, H.; Qu, X.; Zhao, C.; Shi, Y.; Guo, L.; Yuan, Z. *Zhongguo Zhongyao Zazhi (Chin. J. Chin. Mat. Med.)* **1995**, *20*, 115–6, 128.

(3) Leboul, J.; Provost, J. French Patent WO96/00205, 1996; *Chem. Abstr.* **1996**, *124*, 242296.

(4) The substructure search was done on fragment **i** in the Beilstein Commander database.

**i**

(5) Murray, D. F.; Baum, M. W.; Jones, M., Jr. *J. Org. Chem.* **1986**, *51*, 1–7.

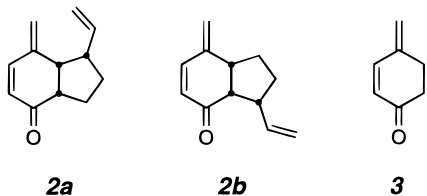
(6) (a) Birch, A. J. *J. Proc. R. Soc. N. S. W.* **1949**, *83*, 245. (b) Jung, M. E.; Rayle, H. L. *Synth. Commun.* **1994**, *24*, 197–203. (c) Wild, H. *J. Org. Chem.* **1994**, *59*, 2748–2761.

[†] Mansoura University.

[‡] Department of Chemistry, University of Minnesota.

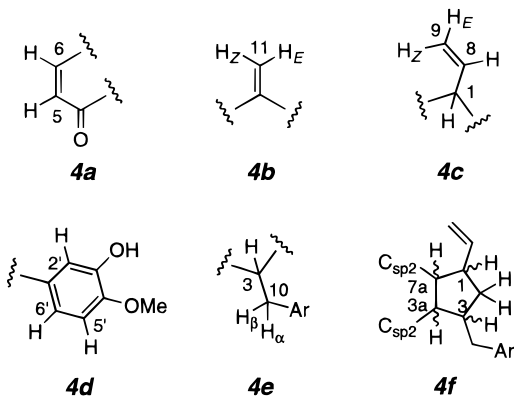
[§] Department of Medicinal Chemistry, University of Minnesota.

(1) Tackholm, V. *Students' flora of Egypt*; Cairo University Press: Cairo, 1974; p 888.



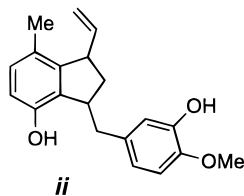
leukemia cell line (P388/DOX) with a GI₅₀ of 1 ng/mL (3 nM).³ We observed growth inhibition of two murine tumor cell lines (NIH3T3 and SSVNIH3T3) by purified samples of both **1A** and **1B** at <0.05 μg/mL (<200 nM). We then submitted both ottelione A and ottelione B to the National Cancer Institute Developmental Therapeutics in vitro screening program against a panel of ~60 human tumor cell lines. Both compounds reproducibly show remarkable levels of cytotoxicity. For example, ottelione A (**1A**) showed GI₅₀'s of <100 pM and ottelione B (**1B**) of <1 nM for most cell lines. Selective total growth inhibition (TGI) was observed against several cell lines; **1A** and **1B** showed TGI values of <100 pM and 3 nM, respectively, against one breast cancer (MDA-MB-435) and of <100 pM and <1 nM, respectively, against one CNS cancer (SF-539) cell line. The complete set of data from the NCI screens is included as Supporting Information.

The proton NMR chemical shifts and ¹H–¹H COSY interactions for each of otteliones A and B are listed in Table 1. Each gave a clear indication for the presence of the set of structural subunits **4a–f**. This accounts for



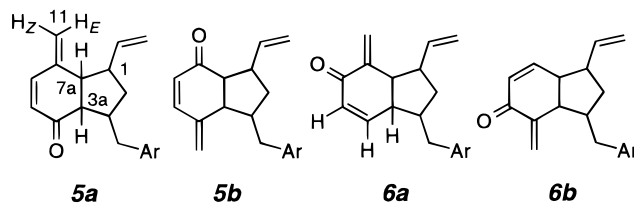
all of the carbons observed in the ¹³C NMR spectra of **1A** and **1B** and is consistent with the molecular formula of C₂₀H₂₂O₃ indicated by the high-resolution mass spectrum of each. The skeletal numbering in these fragments corresponds to that of the fully constituted natural product structure. The α,β-unsaturated ketone fragment **4a** was suggested by resonances at δ ~5.9 (d, *J* ≈ 10 Hz) and ~7.0 (d, *J* ≈ 10 Hz) in the ¹H NMR spectrum and bands at 1657 and 1675 cm⁻¹ in its infrared spectrum. The *exo*-methylene fragment **4b** was indicated by a pair

(7) It is relevant that isomer **ii** was isolated along with **1A** from the *Ottelia* extracts by the Rhone-Poulenc Rorer group.³ We did not detect any *p*-cresol compounds in our crude extracts.



of broad singlets at δ ~5.3–5.4. The allylicly branched, terminal vinyl moiety **4c** was divulged by the classic set of four-spin multiplets for protons H(9*E*), H(9*Z*), H(8), and H(1). The 3,4-dioxygenated phenyl substituent **4d** was suggested by the chemical shifts and coupling values of three aromatic protons in each of **1A** and **1B**. A gradient nuclear Overhauser effect (gNOE) experiment was performed on each isomer to deduce the location of the methyl ether and phenolic hydroxyl groups. Irradiation of the methyl resonance enhanced only the H(5') multiplet in each, which is unambiguously distinguished from H(6') by the lack of meta coupling present in the resonance for the latter (*J*_{2'/6'} = 1.9/2.0 Hz). The presence of the β-branched benzylic three-spin system in subunit **4e** was clear from the pair of ABX resonances for the benzylic protons at δ ~3.1 and ~2.4. Finally, and importantly, the presence of a cyclopentane ring substituted as shown in **4f** was deduced from careful analysis of the COSY spectra and vicinal coupling constants, which showed this closed array for each compound.

From the high-resolution mass and ¹³C NMR spectra for each of **1A** and **1B**, it was clear that the intact molecular constitution could be assembled by joining fragments **4a**, **4b**, and **4f** with no additional atoms. Of the four possible skeletons **5a/b–6a/b**, only **5a** was consistent with the coupling data for the bridgehead methine protons H(7a) and H(3a). The former, H(7a), the location of which is clearly identifiable from its vicinal coupling to the allylic proton H(1), shows long-range allylic coupling to each of the two *exo*-methylene protons at C(11). This fact rules out possibilities **5b** and **6b**.



Alternative skeleton **6a** was discarded and **5a** established by the lack of any observable coupling between proton H(3a) and either of the vinylic protons associated with the α,β-unsaturated enone unit. A subsequent NOESY experiment verified this conclusion by showing the proximity of H(6) and H(11*Z*). A search of the literature for related molecules led us to the report of the Rhone-Poulenc Rorer group, in which the isolation, constitution, and biological activity of **1A**, also isolated from *O. alismoides*, was described. The relative configuration of the four stereocenters was not discussed, nor was the second isomer **1B** reported.

Having established that **5a** is the constitution of both otteliones A and B, we turned to the analysis of their relative configuration. The assigned coupling constants for each of **1A** and **1B** are summarized in the first column of Tables 3 and 2, respectively. We assumed that **1B** contained a *trans* ring fusion and **1A** a *cis* ring fusion because *J*_{3a/7a} was 14.1 Hz in the former isomer and 8.1 Hz in the latter. However, stereochemical assignments of flexible, substituted cyclopentane rings are notoriously difficult to deduce from coupling constant data alone because of the frequent presence of energetically similar ring conformations. We elected to use molecular modeling to compute coupling constants for comparison with the experimental *J* values. Thus, the family of cyclo-

Table 1. Proton Chemical Shifts (in CDCl₃ and C₆D₆) and ¹H–¹H COSY Interactions for 1A and 1B

proton	ottelione A (1A)			ottelione B (1B)		
	δ CDCl ₃	δ C ₆ D ₆	COSY ^{a(x)} ^b	δ CDCl ₃	δ C ₆ D ₆	COSY ^{a(x)} ^b
H(1)	2.62	2.35	2α, 2β, 7α, 8, 9	2.73	2.32	2α, 2β, 7α, 8, 9
H(2α)	1.76	1.65	1, 2α, 3	1.78	1.55	1, 2α, 3
H(2β)	1.57	1.36	1, 2β, 3	1.57	1.32	1, 2β, 3
H(3)	2.51	2.20	2α, 2β, 3a, 10α, 10β	2.50	2.42	2α, 2β, 3a, 10α, 10β
H(3a)	2.86	2.44	3, 7a	2.27	1.94	3, 7a
H(5)	5.93	5.77	6	5.94	5.82	6
H(6)	6.98	6.30	5	7.00	6.39	5
H(7a)	2.78	2.17	1, 3a	2.52	2.09	1, 3a
H(8)	5.76	5.39	1, 9E, 9Z	5.73	5.38	1, 9E, 9Z
H(9E)	4.97	4.80	1, 8, 9Z	4.99	4.80	8, 9Z
H(9Z)	4.93	4.70	1, 8, 9E	5.09	4.82	8, 9E
H(10α)	3.05	3.41	3, 10β	3.15	3.28	3, 10β
H(10β)	2.49	2.69	3, 10α	2.34	2.19	3, 10α
H(11E)	5.32	4.89		5.44	5.18	
H(11Z)	5.31	4.81		5.30	4.84	
H(2')	6.78	7.03	6'	6.80	7.03	6'
H(5')	6.75	6.40	6'	6.77	6.42	6'
H(6')	6.68	6.78	5', 2'	6.69	6.72	5', 2'
OCH ₃	3.86	3.12		3.86	3.11	
OH	5.53	5.42		5.53	5.42	

^a COSY spectra were recorded in C₆D₆. ^b Correlations observed to protons H(x).

Table 2. Observed Coupling Constants for Trans Isomer 1B and Calculated J's for Diastereomers 7–10

coupling constants (in Hz)					
	observed J's ^a	calculated vicinal J's	calculated vicinal J's	calculated vicinal J's	calculated vicinal J's
J _{1,2α}	9.9 ^b	7.5	1.4	9.0	9.7
J _{1,2β}	8.1 ^b	9.7	8.6	8.4	6.2
J _{1,7a}	10.4	11.8	5.2	11.7	5.0
J _{1,8}	8.2	8.6	9.1	8.6	9.6
J _{2α,3}	6.8 ^b	2.0	5.1	6.8	9.7
J _{2β,3}	10.0 ^b	4.9	9.9	9.7	6.2
J _{3,3a}	10.0	7.6	10.4	11.3	8.6
J _{3,10α/10β}	3.5 and 10.3	3.6 and 11.7	5.9 and 8.5	4.2 and 10.3	4.0 and 11.7
J _{3a,7a}	14.1	12.5	12.5	12.5	12.5
chi-squared (χ ²) ^c		59	116	10	66

^a Non-calculable J_{obs}'s: J_{2α,2β} = 13.6, J_{5,6} = 9.8, J_{7a,11E} = ~1, J_{7a,11Z} = ~1, J_{8,9E} = 10.1, J_{8,9Z} = 17.3, J_{10α,10β} = 13.4, J_{11E,11Z} = ~1, J_{2',6'} = 2.1, and J_{5',6'} = 8.2.

^b On the basis of coupling constants alone the assignment of resonances to protons H_{2α} and H_{2β} was uncertain. The nOe experiments (see text) permitted the definitive assignment; since both H(2β) and H(7a) were enhanced by irradiation of H(8), they must be cis-disposed on the cyclopentane ring.

^c χ² = Σ (J_{obs} - J_{calc})².

pentane conformations available to each of the eight diastereomers (7–10 for the trans-fused and 11–14 for the cis-fused series) that exists for skeleton 5a (Ar = Ph) was identified. A Monte Carlo-based conformational search using the MM2* force field as implemented in MacroModel⁸ (v6.0) generated a conformer family containing all geometries within 50 kJ/mol of the global minimum for each of the diastereomers. The Boltzmann

weighted, calculated, vicinal coupling constants for 7–10 and 11–14, which are listed in the final four columns of Tables 2 and 3, were then compared with the set of observed J's for each of the diastereomers 1B and 1A.

There is remarkable consistency in the calculated vicinal coupling constant between protons H(3a) and H(7a) within each family of trans- and cis-fused compounds. Each of the trans-fused isomers 7–10 has a J_{3a,7a} = 12.5 Hz, while the J_{3a,7a} values for the cis-fused set 11–14 range from 7.2 to 8.5 Hz. These compare favorably with the experimental values of 14.1 and 8.1

(8) Mohamadi, F.; Richards, N. G. J.; Guida, W. C.; Liskamp, R.; Lipton, M.; Caufield, C.; Chang, G.; Hendrickson, T.; Still, W. C. *J. Comput. Chem.* **1990**, *11*, 440–467.

Table 3. Observed Coupling Constants for Ottelione A (1A) and Calculated J's for Diastereomers 11–14

coupling constants (in Hz)	1A	11	12	13	14
	observed vicinal J's ^a	calculated vicinal J's	calculated vicinal J's	calculated vicinal J's	calculated vicinal J's
J _{1,2α}	6.4 ^b (or 7.6) ^c	4.9	10.3	6.0	1.6
J _{1,2β}	9.5 ^a	11.9	7.3	7.7	5.9
J _{1,7a}	9.0	11.8	8.5	5.2	5.8
J _{1,8}	8.2	9.2	8.3	7.8	10.0
J _{2α,3}	7.6 ^b (or 6.4) ^c	7.4	11.3	4.2	7.0
J _{2β,3}	9.5 ^a	10.2	5.6	6.6	10.3
J _{3,3a}	5	5.4	5.8	7.7	5.8
J _{3,10α/10β}	7 and 9	6.1 and 8.4	4.2 and 10.6	4.7 and 10.9	5.8 and 8.7
J _{3a,7a}	8.1	8.0	7.2	8.3	8.5
	chi-squared (χ ²) ^d	19	18	51	53

^a Non-calculable J_{obs} 's: $J_{2\alpha,2\beta} = 13.1$, $J_{5,6} = 10.1$, $J_{7a,11E} = -1$, $J_{7a,11Z} = -1$, $J_{8,9E} = 10.0$, $J_{8,9Z} = 16.9$, $J_{10\alpha,10\beta} = 13.5$, $J_{11E,11Z} = -1$, $J_{2',6'} = 2.1$, and $J_{5',6'} = 8.1$.

^b The assignment of resonances to protons H_{2α} and H_{2β} was uncertain. Therefore, the J values for both pairs of J_{1,2} and J_{2,3} may be interchanged.

^c The multiplets for both H(1) and H(3) are too complex to distinguish whether they contain a 6.4 or 7.6 Hz coupling to one of the diastereotopic protons at C(2).

^d The indicated χ^2 values represent the best fit for the calculated data set to any of the four possible^{b,c} experimental sets.

Hz for **1B** and **1A**, respectively, thereby reinforcing the initial hypothesis that the ring-fusion geometries of the two otteliones are different.

To define the remaining stereocenters in the trans-fused isomer **1B** (Table 2) we compared the remaining observed vicinal coupling constants with those calculated for each of the possible diastereomers **7–10**. It is clear even from visual inspection of the numerical data that the set of J_{calc} 's for isomer **9** best fits the set of J_{obs} 's for **1B**. To make this a more objective exercise, we examined the sums of the squares of the differences [i.e., $\chi^2 = \sum (J_{\text{obs}} - J_{\text{calc}})^2$] across the entire set of observed vs calculated coupling constants. χ^2 is the same statistical parameter that is used in least-squares analysis to determine goodness of fit. Again, isomer **9** ($\chi^2 = 10$) shows the best correlation among any of **7**, **8**, or **10** ($\chi^2 = 59$, 116, or 166, respectively). Therefore, the molecular modeling study suggests the relative configuration (1 α ,3 β ,-3a β ,7a α) for ottelione B.

That ottelione B (**1B**) has the relative configuration of **9** is confirmed by key sets of NOE's that were observed in **1B** and that are shown by the arrows in Figure 1. Namely, the vinylic proton H(8) enhances protons H(7a) and H(2 β) and the bridgehead methine proton H(3a) enhances the H(10a) benzylic protons. Additionally, the diastereomeric benzylic proton, H(10b), shows a NOESY correlation to H(2 α). The combination of these NOE's demands that the trans-fused ottelione B (**1B**) has the relative configuration shown in Figure 1. Incidentally,

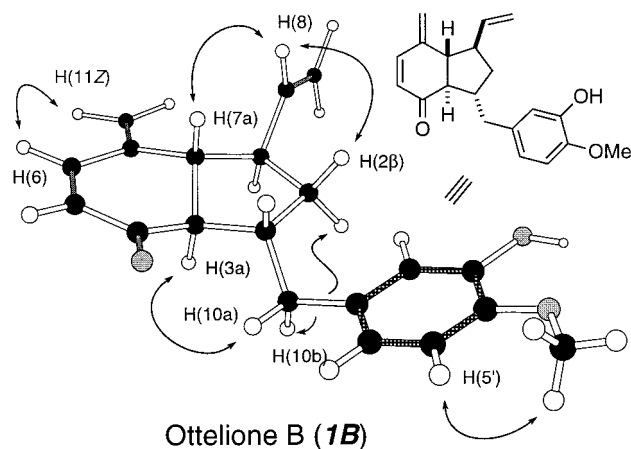


Figure 1. Key NOE's and relative configuration assigned for ottelione B (**1B**).

the NOE between H(6) and H(11Z) is consistent only with the earlier assigned constitution **5a** (*vis-à-vis* **5a**, **6a**, and **6b**).

The relative configuration of ottelione A **1A** could not be uniquely defined. Unlike the case with **1B**, resonances for diastereotopic protons H(2 α) and H(2 β) could not be distinguished. The analysis was further complicated by the fact that the multiplets for H(1) and H(3) were too complex to distinguish which contains a 6.4 or 7.6 Hz coupling to one of the diastereotopic protons at C(2). These ambiguities required us to compare four possible

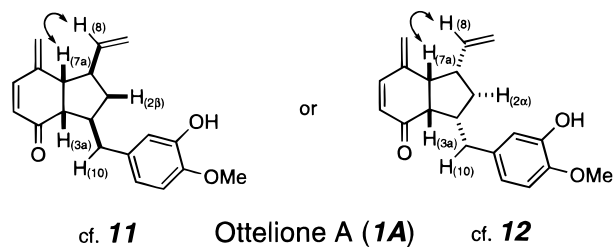


Figure 2. Ottelione A (**1A**).

sets of the observed vicinal coupling constants to each set of those calculated for the possible diastereomers **11**–**14** (see Table 3, footnotes b–d). Visual comparison of the data sets no longer permits an obvious assignment. The χ^2 's for each isomer fall within a narrow range (18–53) and point to two possible configurational assignments of essentially equal quality [i.e., **11** ($\chi^2 = 19$) and **12** ($\chi^2 = 18$)]. Thus, the molecular modeling studies suggest that the C(1) and C(3) appendages to the cyclopentane ring in ottelione A (**1A**) are either both syn or both anti to the cis-oriented bridgehead protons H(3a) and H(7a).

The NOE study of ottelione A (**1A**) revealed the proximity of protons H(8) and H(7a) (Figure 2). No other definitive enhancements [e.g., between proton pairs H(3a)/H(10) or H(8)/H(2 β or α)/H(10)] were detected. Most of the various MacroModel-derived conformations of **11** (Table 3) bring these two protons into close proximity. While it is tempting to use these observations to argue that **1A** has the relative configuration of **11**, it is also true that isomer **12** has a few minor conformations within its population that might permit magnetization transfer ($d_{[H(7a)-H(8)]} \leq 4 \text{ \AA}$). Therefore, we tentatively assign the (1 α ,3 α ,3 $\alpha\alpha$,7 $\alpha\alpha$) configuration (i.e., **11**) to ottelione A but cannot confidently rule out the alternative configuration of structure **12** (1 α ,3 α ,3 $\alpha\beta$,7 $\alpha\beta$). We are currently pursuing a total synthesis of ottelione A in order to rigorously establish its relative (and absolute) configuration.

Experimental Section

1-Ethenyl-1,2,3,3a,7,7a-hexahydro-3-[(3-hydroxy-4-methoxyphenyl)methyl]-7-methylene-4H-inden-4-ones **1A and **1B**.** Whole plants of *O. alismoides* (1 kg) that had been air-dried and protected from light were exhaustively extracted

with cyclohexane (15 L). The combined organic extracts were concentrated under vacuum to give a dark green residue (30 g). The residue was chromatographed on silica gel (400 g, 90 \times 5 cm), eluting first with cyclohexane followed by a gradient of cyclohexane/ether. The fraction eluted with cyclohexane/ether (1:1) was concentrated and further purified by flash chromatography on silica gel (benzene/ethyl acetate 4:1). The fractions containing compounds with an $R_f = 0.44$ (benzene/ethyl acetate 4:1) were collected and concentrated to give 160 mg of crude **1A** and **1B**. The compounds were then separated by preparative thin-layer chromatography (preparative TLC) on SiO₂ plates eluting with hexanes/ethyl acetate (5:2) to give **1A** (9 mg, $R_f = 0.30$) and **1B** (9 mg, $R_f = 0.27$). **1A**: ¹H NMR (500 MHz, see Tables 1 and 3); ¹³C NMR (CDCl₃, 75 MHz) δ 200.5 (C_{quat}), 146.0 (CH), 145.4 (C_{quat}), 144.8 (C_{quat}), 143.0 (C_{quat}), 141.9 (CH), 135.2 (C_{quat}), 128.4 (CH), 120.3 (CH), 119.9 (CH₂), 115.0 (CH), 114.4 (CH₂), 110.6 (CH), 55.9 (CH₃), 51.5 (CH), 49.1 (CH), 48.6 (CH), 46.4 (CH), 35.8 (CH₂), 35.6 (CH₂); IR (thin film) 3371, 2920, 2851, 1735, 1657, 1510, 1262, 1128, 1028, 910, 800 cm⁻¹; GC/MS [70 eV, *m/e* (rel int)] 310 (15), 256 (13), 203 (5), 173 (3), 171 (3), 163 (7), 161 (14), 137 (32), 107 (100, C₇H₇O); HRMS calcd for C₂₀H₂₂O₃ 310.1569, found 310.1571. **1B**: ¹H NMR (500 MHz, see Tables 1 and 2); ¹³C NMR (CDCl₃, 75 MHz) δ 200.6 (C_{quat}), 147.6 (CH), 145.4 (C_{quat}), 144.9 (C_{quat}), 142.9 (C_{quat}), 141.6 (CH), 134.2 (C_{quat}), 128.8 (CH), 120.5 (CH), 117.2 (CH₂), 115.5 (CH), 114.9 (CH₂), 110.6 (CH), 58.4 (CH), 56.0 (CH₃), 50.6 (CH), 45.6 (CH), 40.7 (CH₂), 38.0 (CH), 37.0 (CH₂); IR (thin film) 3371, 2925, 2852, 1736, 1675, 1510, 1273, 1128, 1029, 914, 804 cm⁻¹; GC/MS [70 eV, *m/e* (rel int)] 310 (37), 256 (6), 203 (4), 173 (18), 171 (6), 163 (8), 161 (13), 137 (64), 107 (100); HRMS calcd for C₂₀H₂₂O₃ 310.1569, found 310.1566.

Acknowledgment. We thank Dr. A. A. Khedr, Botany Department, Faculty of Science, Mansoura University, New Damietta, Egypt, for identification and collection of *O. alismoides*. This research was supported by Research Project Grant DHP-140 from The American Cancer Society, and more recently, by the National Institutes of Health (CA-76497).

Supporting Information Available: Results from two separate assays for each of **1A** and **1B** in the National Cancer Institute Developmental Therapeutics Program in vitro anti-tumor screens against ~60 individual human tumor cell lines (16 pages). This material is contained in libraries on microfiche, immediately follows this article in the microfilm version of the journal, and can be ordered from the ACS; see any current masthead page for ordering information.

JO971870A